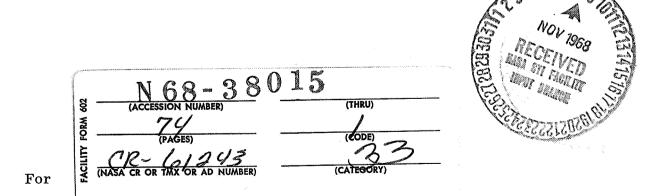NASA CONTRACTOR
REPORT

NASA CR-61243

August 1968

SURFACE EFFECTS RESULTING FROM TEKTITE ABLATION

Prepared under Contract No. NAS 8-20082 by
LOCKHEED MISSILES AND SPACE COMPANY

For

NASA-GEORGE C. MARSHALL SPACE FLIGHT CENTER
Marshall Space Flight Center, Alabama

SURFACE EFFECTS RESULTING FROM TEKTITE ABLATION

By

J. O. Golden and M. L. Blackledge

Prepared under Contract No. NAS 8-20082 by

LOCKHEED MISSILES AND SPACE COMPANY
Huntsville, Alabama

For

Aero-Astrodynamics Laboratory

NASA-GEORGE C. MARSHALL SPACE FLIGHT CENTER

FOREWORD

This report presents the results of work performed by
Lockheed's Huntsville Research & Engineering Center while
under subcontract to Northrop Nortronics (NSL PO 5-09287)
for the Aero-Astrodynamics Laboratory of Marshall Space
Flight Center (MSFC), Contract NAS8-20082. This task was
conducted in response to the requirement of Appendix B-1
Schedule Order No. 66.

Acknowledgement is extended to the following personnel:
Dr. John A. O'Keefe, Research Studies Laboratory, Goddard
Space Flight Center; Mr. Milton Huffaker, Technical Coordinator,
Thermal Environment Branch, Aero-Astrodynamics Laboratory,
Marshall Space Flight Center; and Mr. Charles P. Verschoore,
Vehicle Components and Sub-systems Branch, Test Laboratory,
Marshall Space Flight Center.

SUMMARY

Results are presented of an experimental investigation to evaluate the types of surface structure produced during the ablation of tektite materials in the exhaust plume of small rocket test engines. Motivation for this study was supplied by the desire to reproduce with ablation tests the grooving and pitting found on certain classes of natural tektite materials. Positive results would then be an additional verification of the parent body hypothesis for tektite origin.

A series of ablation tests, including firings on both natural and synthetic tektite materials, was conducted in the exhaust plumes of rocket test engines fueled with liquid oxygen/hydrogen and liquid oxygen/kerosene. The surface structure features produced on the tektite material were then compared to those found on natural tektites. Photographic results of these tests are presented in this report. In addition, high-speed photography was used to evaluate the surface structure during the actual ablation experiments.

PRECEDING PAGE BLANK NOT FILMED.

CONTENTS

LIST OF FIGURES

LIST OF FIGURES (Continued)

LIST OF FIGURES (Continued)

LIST OF TABLES

Section 1
INTRODUCTION

The origin of tektite materials has long been discussed by scientists throughout the world. A number of theories have been advanced that favor both terrestrial and extraterrestrial origin of these materials. Arguments for both origins have been presented on the basis of physical, geological, geographic, chemical and aerodynamic phenomena. These arguments are well summarized by Dr. John A. O'Keefe (Reference 1).

If one accepts the theory of extraterrestrial origin, and further that the original source of tektite materials was the lunar surface (a theory under serious consideration), two possible methods of earth arrival may be explored. The first method involves direct arrival from the Moon and has been proposed by D. R. Chapman and his co-workers (References 2 and 3). The second method considers the parent body hypothesis and involves the idea that tektites are ablation droplets from an orbiting satellite which eventually entered the earth's atmosphere. This theory was originally proposed by F. E. Suess (Reference 4) and has been further amplified by Hanus (Reference 5), O'Keefe and Shute (Reference 6) and Adams and Huffaker (Reference 7).

A careful examination of the parent body hypothesis for extraterrestrial origin is complex and involves orbital mechanics, trajectory analysis and ablation phenomena. The salient feature of this hypothesis as applied to the present investigation, however, involves the proposition that tektite materials would result from the parent body entering the Earth's atmosphere. The important feature is that ablation of certain tektite materials would occur in the relatively dense lower atmosphere, as opposed to ablation that would occur at much higher altitudes for tektites entering the Earth's atmosphere upon direct arrival from the Moon.

The purpose of this investigation, therefore, was to examine the surface effects produced upon ablation of tektite materials in a relatively high density environment, such as that of the exhaust plume of small scale rocket engines. The motivation for this study was supplied by the fact that certain tektite materials (splash form tektites) exhibit surface structure (pitting and grooving) that has not been reproduced in the laboratory. If pitting and grooving on natural tektite materials could be shown to be the result of aerodynamic ablation phenomena in a dense gas stream, then an additional basis of support could be established for the parent body hypothesis.

Further motivation for this study was prompted by the fact that early efforts to test materials for use as heat shields resulted in pitting and grooving much like that found in natural tektites. Therefore, as a result of a suggestion by Dr. O'Keefe, tests were initiated to examine the type of surface structure produced in the ablation of both natural and synthetic tektite materials in the plume of a small rocket engine.

A description of the experimental program is presented in the following section of this report.

Section 2

EXPERIMENTAL PROGRAM

The experimental program was conducted in two phases:

Phase I Preliminary Investigation of the Ablation of Natural and Synthetic Materials in a LOX/RP Engine Exhaust Plume

Phase II Detailed Investigation of the Ablation of Synthetic Materials in a LOX/H_2 Engine Exhaust Plume.

A discussion of the test program and experimental results for Phase I follows:

2.1 PHASE I TEST PROGRAM

The objective of Phase I was to evaluate the potential worth of a more detailed investigation of the surface effects produced during ablation of natural and synthetic tektite samples.

2.1.1 Test Engine

For these tests, a LOX/RP engine was selected for producing the test environment on the basis of convenience. Even though the combustion products of LOX/RP are complex and could be called somewhat "chemically dirty," a LOX/RP engine was selected because it was dependable and more convenient to use in comparison to a somewhat "chemically clean" LOX/H_2 engine.

The LOX/RP engine data used in Phase I are given in Table 1.

Table 1

LOX/RP ENGINE CHARACTERISTICS

Engine	1/20-scale F-1
Nominal Thrust	4000 lb
Throat Diameter	1,744 in.
Exit Diameter	7.0 in
Nominal Expansion	16:1
Nozzle Half Angle	17° 34'
Approximate Time from Ignition to Steady-State Operation	0.6 sec.

2.1.2 Test Plan

The Phase I test plan was as follows:

1. Solve the problems of mounting a fragile glass sample in a high density supersonic plume flow field.

2. Evaluate the surface structure effects produced by the ablation of natural tektite samples (rough initial surface).

3. Evaluate the surface structure effects produced by the ablation of synthetic tektite samples with small holes drilled in an otherwise smooth surface. (The goal here was to investigate the growth or decay of a pit on the sample surface during ablation of the sample.)

As was expected, a satisfactory solution to the sample-mounting problem required several tests before a sample could be recovered or partially recovered after the tests. Basically, a satisfactory mount design involved making a small nipple and flange on the tektite sample and bonding the tektite with epoxy to a stainless steel sting. Even with this system, the probability existed of losing a sample (bond melting and the sample falling to the ground) on a given run.

Approximately six tests were conducted during Phase I. Only two tests, however, produced meaningful results. The other tests were involved in solving the problem of mounting the sample or resulted in no useful sample being recovered.

2.1.3 Test Conditions and Results

● Test 171-23

The material used in this test was a flat natural tektite with one side machined to fit the mounting system. The other side (natural surface) was cleaned before the test by lightly brushing the surface to remove contamination. Figure 1 shows the prepared sample prior to the test. Sample diameter and weight were 1.6 inches and 25.3 grams after machining. The sample was located 15 inches from the nozzle exit plane for the test (see Figure 2). Pertinent engine operating conditions are given in Table 2.

Table 2

ENGINE OPERATING CONDITIONS

Chamber pressure	1006 psia
LOX flow	9.04 lb/sec
Fuel flow	4.99 lb/sec
O/F ratio	1.81
Specific impulse	256.6 sec
Estimated combustion temperature	5500°R
Estimated nozzle exit pressure	6.8 psia
Estimated nozzle exit temperature	2000°R
Engine run time	2.0 sec

Figure 3 is a photograph taken during the actual ablation test. Notice the normal shock region immediately in front of the sample. For this test the sample was positioned sufficiently far downstream from the nozzle exit plane such that a number of Mach discs (shock diamonds) existed in the plume between the nozzle and the sample. The flow was supersonic just ahead of the

Mach disc and then would shock down to subsonic flow after crossing a normal shock. Also, the growth of a free shear layer from the nozzle lip would make the results obtained somewhat hard to interpret.

Theoretical calculation of plume flow fields involving more than one Mach disc is difficult. Flowfield calculations using a real gas method of characteristics flow solution, however, were used up to the location of the Mach disc. This was followed with approximate one-dimensional techniques downstream of the Mach disc which yielded the following results for freestream flow conditions at the sample location:

Mach Number	2.87
Pressure	1.55×10^1 psia (1.06×10^5 N/m^2)
Density	3.15×10^{-4} slugs/ft^3 (1.62×10^{-1} kg/m^3)
Temperature	2.81×10^3 °R (1.56×10^3 °K)
Velocity	8.56×10^3 ft/sec (2.61×10^3 m/sec).

Figures 4 and 5 are photographs of the sample after the test. The crack in the sample resulted from the thermal shock of a gaseous nitrogen engine purge after the test. The sample surface was covered with a light gray material (not found in the tests using LOX/H$_2$) which probably resulted from a reaction of the surface material with hydrocarbon combustion products of the RP fuel. A definite surface pattern is present; however, the deep pits on the original sample are no longer observed.

High-speed photography of the sample during the ablation test resulted in some interesting though not extremely pertinent film.

● Other Tests

Approximately three tests were conducted using a hemispherical synthetic tektite sample with small holes drilled in the surface (stagnation region). The goal was to evaluate whether the small holes would enlarge or disappear during the ablation tests. However, no samples of this type were recovered because either the mounting system failed or the samples shattered during the test. Therefore, no meaningful results were obtained.

2.1.4   Observations and Conclusions

Although Phase I resulted in only one satisfactory ablation sample, portions of the melt layer were recovered from several other tests and the surface structure observed. These observations combined with the successful test were encouraging. Therefore, a more detailed investigation (Phase II) was initiated.

2.2 . PHASE II TEST PROGRAM

The objective of the Phase II experimental program was to conduct a more detailed and systematic investigation of the surface effects produced during the ablation of tektite materials. To this end, a test program was initiated consisting of 11 firings with an engine using LOX/H_2 fuel. Included in this test program were:

- Firings to determine plume geometry and flow fields
- Firings to measure heat flux in the plume, and
- Firings to evaluate tektite ablation effects.

Evaluation of the Phase I study indicated that a primary weakness in the program was a rather undefined test environment (the LOX/RP plume flow field). Therefore, before beginning Phase II, two decisions were reached. First, a "cleaner" LOX/H_2 engine was to be used as the test engine rather than the LOX/RP engine. Secondly, the plume test environment needed to be better defined. Plume definition was achieved through a series of tests to photographically determine plume geometry and Mach disc location prior to the ablation tests. A detailed analytic effort was made to define the flow field. The results of this effort are presented in Appendix A.

2.2.1   Test Engine

For Phase II, a 1200-lb thrust LOX/H_2 engine was used to produce the test environment. Pertinent engine data are given in Table 3.

Table 3

LOX/H_2 ENGINE CHARACTERISTICS

Engine	Scaled J-2
Nominal Thrust	490 lb to 1140 lb
Chamber Pressure	350 to 750 psia
Throat Diameter	1.2 in.
Exit Diameter	3.5 in.
Nominal Expansion	8.5:1
Nozzle Half Angle	18 deg
Approximate Time from Engine Ignition to Steady-State Operation	1.5 sec
Approximate Time from Engine Ignition to Deflector Removal	1.75 sec

The flow field analysis of Appendix A yielded the following freestream conditions at the sample location:

Chamber Pressure
= 350 psia
(2.41×10^6 N/m^2)

Mach Number	2.23
Pressure	2.56×10^1 psia (1.76×10^5 N/m^2)
Density	2.15×10^{-4} slugs/ft^3 (1.11×10^{-1} kg/m^3)
Temperature	4.49×10^3 °R (2.49×10^3 °K)
Velocity	9.98×10^3 ft/sec (3.04×10^3 m/sec)

Chamber Pressure
= 750 psia
(5.16×10^6 N/m^2)

Mach Number	4.01
Pressure	2.19 psia (1.51×10^4 N/m^2)
Density	3.35×10^{-5} slugs/ft^3 (1.73×10^{-2} kg/m^3)
Temperature	2.48×10^3 (1.38×10^3 °K)
Velocity	1.38×10^4 ft/sec (4.20×10^3 m/sec)

One fact concerning engine startup is worthy of comment. The igniter system for the LOX/H$_2$ engine employed tetraethylaluminum (TEA), which was potentially very damaging to the tektite samples. Therefore, the samples had to be protected during engine startup with a shield or flame deflector. (See Figure 6 which shows the test engine, flame deflector and sample sting.) The flame deflector, operated pneumatically, could respond in less than one second. On engine startup, the sample would be protected by the flame deflector. On a given command (after the flow of TEA had stopped), the deflector would drop rapidly downward, remain for the given sample exposure time, and then return to its original position of sample protection.

Although the flame deflector was necessary, its use resulted in two problems that plagued the ablation tests. First, the rapid pneumatic action resulted in moderate sting oscillation which was discovered only after examining high-speed movies of the initial test. On several early tests, removal of the oscillation was attempted by reinforcing of the mounting system. The oscillation, however, remained throughout the investigation. Secondly, the mechanics of the flame deflector and sting-mounting system made proper alignment of the sample very difficult. A slight misalignment resulted in asymmetric flow over the sample. Asymmetric flow was observed on most tests.

In addition, it was recognized before the tests that use of the flame deflector would result in asymmetric flow field just by virtue of its movement in front of the sample before and after the ablation test. This was sufficient to give asymmetrical heating rate distributions over the sample for the initial and final portions of the ablation test.

2.2.2   Test Plan

The test plan for the Phase II investigation was as follows:

1. Photographically define plume geometry and Mach disc locations by a series of firings at various engine chamber pressures. (Chamber pressure was the primary engine variable controlling plume geometry for fixed nozzle geometry and oxidizer/fuel (O/F) ratio.)

2. Perform a series of ablation tests with the samples located between the first Mach disc and the nozzle exit plane. (The goal was to have a flow field as uniform and defined as possible.)

3. Calorimetrically determine the heating rate at pertinent plume locations. (This information would then be used to evaluate heat flux prediction techniques to be used in the ablation studies.)

4. Search for the plume location and conditions that would produce on the synthetic samples the grooving and pitting found on certain classes of natural tektites.

5. All through Steps 1 and 2, analytical flow field and heating rate calculations were performed to support the experimental investigation. In particular, analytical predictions on heating rates were employed to evaluate the thermal environment of proposed sample locations. This information was critical to the design of a successful mounting system.

2.2.3 Test Conditions and Results

A total of eleven experimental firings was conducted during the Phase II investigation. The initial four firings involved only photographic determination of plume geometry. The fifth firing was conducted to obtain experimental measurements of the heat flux for given plume conditions. The remaining six firings were for ablation surface effects studies.

Again, as during the Phase I investigation, sample mounting problems were present. The LOX/H$_2$ engine produced a higher flame temperature than the LOX/RP engine and the samples were extremely close to the nozzle exit plane. Therefore, on a number of runs the sample mounting system failed due to the intense heat of the plume and no usable samples were recovered.

Photographic coverage of the ablation tests involved still photographs and high-speed movie photography of the ablating sample surface. Frequently, either some of the cameras did not function during the tests or the results produced were useless. This problem was not surprising considering the difficulty of photographing an object inside the plume and the complexities of the necessary equipment. Useful and meaningful results, however, were obtained on a number of runs.

Although 11 firings were conducted, only the results of pertinent runs will be presented in the next section.

- Tests 197-1, 2, 3, 4

These four tests will be discussed together since they had the same goal — the determination of plume geometry for given engine operating conditions. The procedure employed here was to take a sequence of photographs during the firing of the engine for a given chamber pressure and O/F ratio. This information would then be used in locating the ablation samples and also in evaluating the theoretical procedures used to calculate the properties of the plume flow field.

The conditions for the four tests were as follows:

Test	Duration (sec)	O/F	Chamber Pressure (psia)
197-1	4.45	4.19	655
197-2	4.94	4.16	710
197-3	6.00	4.34	498
197-4	4.98	6.60	348

On a number of runs duplication of engine performance was requested; however, an exact duplication of the O/F ratio was almost impossible due to the engine feed system of the fuel and oxidizer. These tests, and all subsequent firings, were performed under fuel-rich conditions in an attempt to reduce sample surface and plume chemistry interactions. Selected photographs for Test 197-3 are presented in Figures 7 and 8 while photographs of Test 197-4 are given in Figures 9 and 10. The first Mach disc and alternating supersonic and subsonic regions are clearly visible in Figures 7, 8 and 10. Figure 10 is particularly interesting since six of these regions in sequence can be observed.

For these engine firings, analytical calculations were performed to evaluate the theoretical methods available for predicting plume flowfield

properties. Comparison of plume geometry between that photographed and the geometry predicted theoretically was reasonably good for overall plume description between the nozzle exit plane and the first Mach disc. Precise location of the first Mach disc was difficult analytically and calculations past the Mach disc required approximate techniques.

The tools used in the theoretical plume analysis were a two-dimensional equilibrium real gas method of characteristics computer code (Reference 8, see Appendix A) for both nozzle flow and the inviscid core of the plume. Real gas properties for the LOX/H$_2$ system were generated from the NASA/Lewis Thermochemical Code (Reference 9).

● Test 197-5

The goal of this test was to evaluate the heat flux that the ablation samples would experience during series of tests. Therefore, this test consisted of firing on a calibration model to investigate the stagnation point heating rate encountered in the LOX/H$_2$ plume. The model consisted of a two-inch diameter hemisphere with a standard slug calorimeter placed at the stagnation point (see Figure 11).

The model was positioned 8.75 inches from the nozzle exit plane. Previous analytical calculations (supported by photography) had shown that the first Mach disc would occur about 2.5 inches from the nozzle exit plane. Therefore, the first Mach disc was in front of the model; construction of the flame divider, however, prevented moving the model closer to the nozzle exit plane. (The flame divider was later modified to permit testing closer to the first Mach disc.)

The chamber pressure requested on this calibration run was 350 psia, whereas the measured chamber pressure was 343 psia.

The calorimeter failed during the test; however, fragmentary data indicated that a heating rate of 800 Btu/ft^2-sec was obtained at the stagnation

point. On this test, the problem of correct alignment of the sting and sting oscillation was first noted. Figure 12 shows the asymmetric melting of the sample.

● Test 197-6

This test involved firing on a hemispherical (two-inch diameter) synthetic tektite sample with a very smooth surface which was positioned 8.75 inches from the nozzle exit plane. The engine chamber pressure was 348 psia while the O/F ratio was 7.2 (higher than requested due to flow control difficulties). Although the sample mounting system failed, a usable sample was recovered. Figures 13 and 14 are photographs of the recovered sample. Note the small grooves that extend from the stagnation region to the sides of the sample.

● Test 197-7

The goal of this test was to duplicate the test conditions used on run 197-6 except that a smaller synthetic sample was used (one-inch diameter smooth glass hemisphere). Again, the mounting system failed, but portions of the sample were recovered. Figure 15 shows the sample prior to firing and Figure 16 presents the recovered portions.

● Test 197-8

This test employed a two-inch diameter sample, but had a much higher engine chamber pressure (715 psia) than used previously. The O/F ratio was 6.28 and the mounting system functioned satisfactorily. Figure 17 shows the sample after firing. Note the rather systematic surface structure visible on the sample.

● Test 197-9

This test consisted of firing on a two-inch diameter hemispherical sample. The engine chamber pressure was 745 psia while the O/F ratio was 5.15. Figures 18, 19 and 20 are photographs from various angles for the resulting sample. Note that a large portion of the melt layer chipped off during or after the test.

● Test 197-10

This test again consisted of firing on a two-inch diameter hemispherical synthetic tektite sample. The engine chamber pressure was 740 psia with an O/F ratio of 5.37. Figures 21 through 24 are photographs of the resulting sample from various angles. In this test the asymmetric heating was severe and resulted in a deformed sample, however, the systematic surface structure is again present. Again, a portion of the melt layer was chipped away during or after the test.

● Test 197-11

This test produced no results because the deflector shield failed to operate.

● Test 197-12

The final test in the series was also made on a two-inch diameter specimen. The engine chamber pressure was 723 psia with an O/F ratio of 5.58. Figures 25 through 28 are photographs of the resulting sample from various angles. This is possibly the most interesting sample result- ing from the overall test program. The entire sample is covered with a systematic pattern of grooving and pitting.

Section 3

DISCUSSION OF RESULTS

The discussion of results for both the Phase I and Phase II experimental program will be presented in two sections. The first section will deal with the ablation surface structure produced for the various tests. The next section will deal with a discussion of the findings resulting from high-speed photography of the sample surface during the tests.

3.1 SURFACE STRUCTURE

The results for the Phase I program were interesting and encouraging. In one case, a large flat deeply pitted natural tektite was exposed to a dense, hot gaseous flow field. Figures 4 and 5 show that the pits tended to erode and a rather systematic surface structure was formed. On several other Phase I tests, although no whole sample was recovered, portions of the melt layer of several samples were recovered. The surface structure was somewhat systematic, quite similar to that in Figures 18 and 19. Unfortunately, the chemistry of the LOX/RP plume left a grayish coating on the samples which was not present in the Phase II investigation using a LOX/H$_2$ engine.

The Phase II program also yielded rather interesting results. Although several samples were uninteresting, the rest are worthy of discussion. Test 197-6 (Figures 13 and 14) and Test 197-7 (Figure 16) produced samples that could be termed grooved, that is grooves extended from the stagnation point to the edge of the sample. Test 197-8 (Figure 17) produced a surface structure with a somewhat regular cellular pattern, much like that observed in the test on the natural tektite sample. In Figures 18, 19 and 20 (Test 197-9), both the grooved structure and the cellular pattern are evident. Test 197-10 (Figures 21 through 24), resulted in an asymmetrical sample with a cellular surface pattern. Test 197-12 produced the most interesting sample of the

15

total investigation. Well-defined grooves and surface indentations or pits are evident in Figures 25 through 28.

3.2 HIGH SPEED PHOTOGRAPHY ANALYSIS

On all tests, an attempt was made to utilize high-speed photography of the sample surface to gain some insight into the aerodynamic/thermodynamic development of surface structure during ablation of the samples. Because of the complexities of the photographic equipment and the difficulty in photographing the hot radiating surface through the plume structure, quite often no meaningful film was obtained. Interesting film on three tests, however, was recovered and examined. The interesting effect of mass injection of vapors into the boundary layer was observed along with the shock structure in front of the sample. Only on one set of film was the surface profile or surface structure well defined. In this case the flow pattern of the melt layer was observed along with the formation of the cellular structure shown in several of the after-firing photographs. On most film, the spallation of the sample was easily seen.

Section 4

CONCLUSIONS AND RECOMMENDATIONS

The goal of this study was an evaluation of surface effects produced during the ablation of tektite materials in a rocket nozzle plume. This objective was achieved and the study represents a contribution to the total tektite problem. The investigators recognize the vast effort that presently is and has been devoted to tektite research. Further, many scientific disciplines are required for total comprehension of the problem. Therefore, this study is considered as only a very small portion of the total problem and is presented for evaluation to those familiar with all aspects of the total problem (geochemistry, physics, aerodynamics, geography, etc.). By this reasoning the authors, based on their present knowledge, feel unqualified to reach definite conclusions on the parent body hypothesis.

Results of the study were positive in that certain types of grooving and pitting can definitely be attributed to aerodynamic/thermodynamic phenomena in a dense, hot gas flow field. The nature of the surface structure, however, was not exactly identical to that found on natural tektites. In particular, the deep pits found on certain natural tektites were not present on the investigated samples. It should be pointed out that the investigation was very limited, however, in terms of plume flow conditions where ablation effects were investigated. Further tests might yield more definitive results. In addition, the analytical evaluations of the test conditions were not completed due to level-of-effort considerations and represent a weakness in the study. The flow field for all tests should be calculated and an investigation into the thermal environment of the samples should be performed. Further, these aerodynamic/thermodynamic conditions should be compared with those predicted by the parent body hypothesis.

PRECEDING PAGE BLANK NOT FILMED.

Section 5

REFERENCES

1. O. Keefe, John A., The Origin of Tektites (to be published).

2. Chapman, D. R., Native, Vol. 188, p. 353, 1960.

3. Chapman, D. R., and H. K. Larson, J. Geophysical Research, Vol. 68, p. 4305, 1963.

4. Suess, F. E., Jahrbuch der kk, Reichsanstalt, Vienna, Vol. 50, p. 193, 1900.

5. F. Hanus, Rozpravy Ce ske Akad. Ved a Umeni, Trida II, Vol. 37, 1928.

6. O'Keefe, J. A., and B. E. Shute, Science, Vol. 139, p. 1288, 1963.

7. Adams, E. W., and R. M. Huffaker, Geochem. et. Cosmochem. Acta, Vol. 28, p. 881, 1964.

8. Prozan, R. J., "Development of a Method-of-Characteristics Solution for Supersonic Flow of an Ideal, Frozen or Equilibrium Reacting Gas Mixture," LMSC/HREC A782535, Lockheed Missiles & Space Company, Huntsville, Ala., April 1966.

9. Zeleznik, F. S., and S. Gordon, "A General IBM 704 or 7090 Computer Program for Computation of Chemical Equilibrium Compositions, Rocket Performance, and Chapman-Jouget Detonations," NASA TN D 1454, Lewis Research Center, Cleveland, Ohio, October 1962.

LMSC/HREC A791443

Figure 1 - Test 171-23 (Sample prior to ablation test)
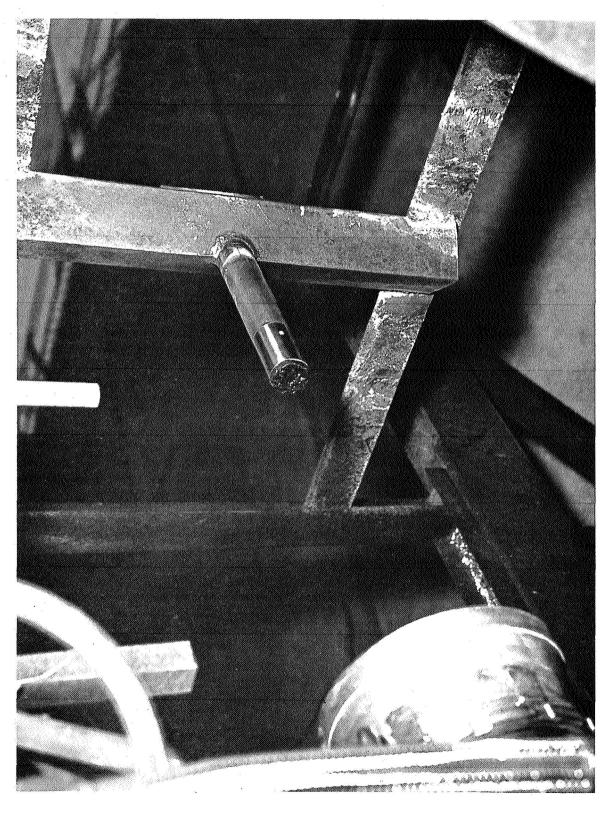
Figure 2 - Test 171-23 (Sample and engine prior to test)
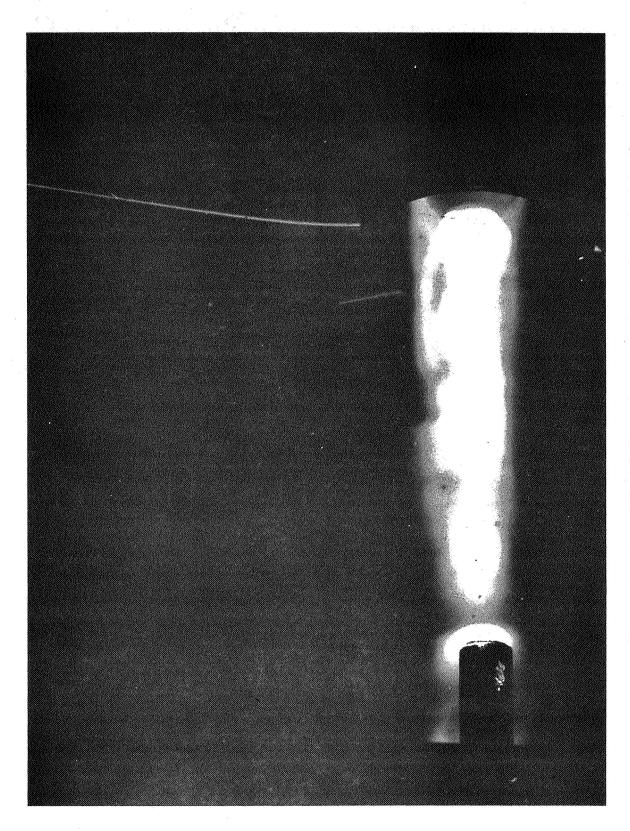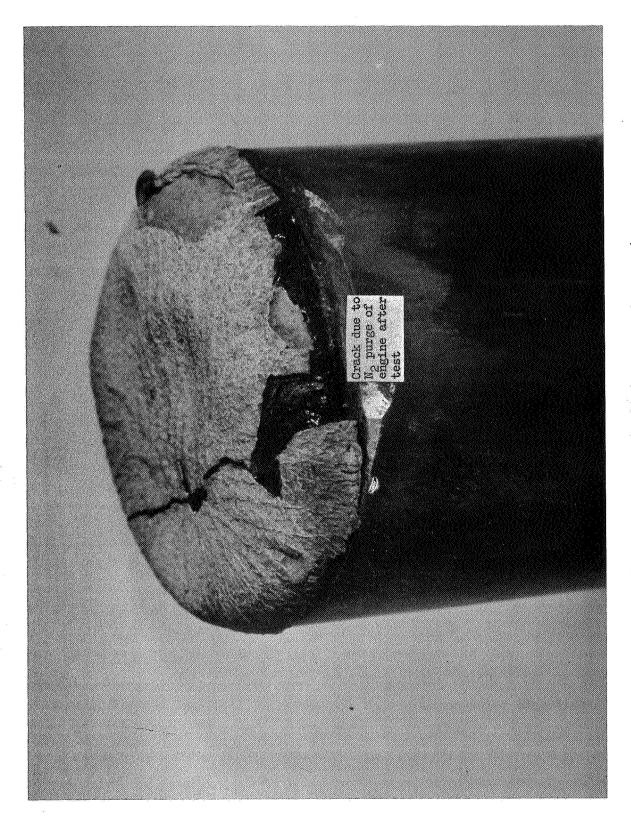
Figure 3 - Test 171-23 (Sample and engine during actual test)

Crack due to
N₂ purge of
engine after
test

Figure 4 - Test 171-23 (Sample after test)

Crack due to N₂ purge of engine after test

Figure 5 - Test 171-23 (Sample after test)
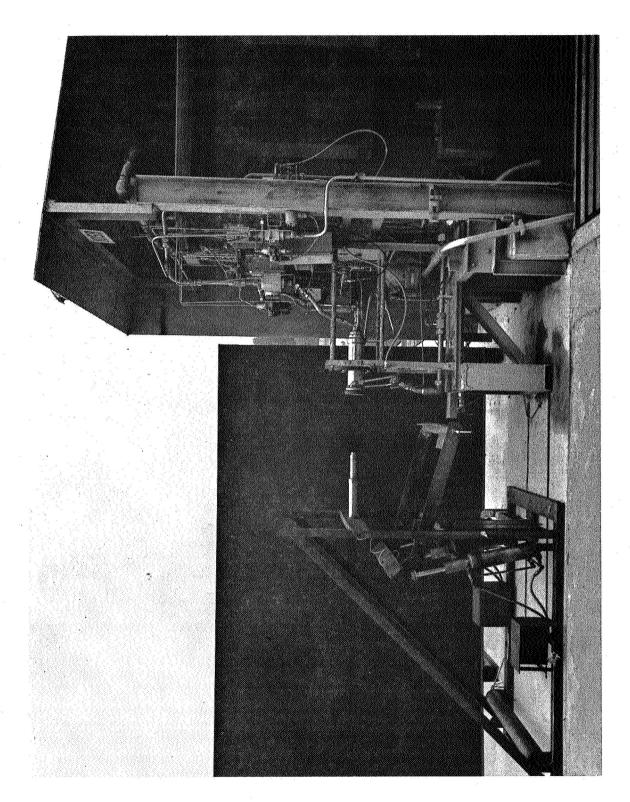
Figure 6 - LOX/H_2 Test Engine, Flame Deflector and Sample Sting
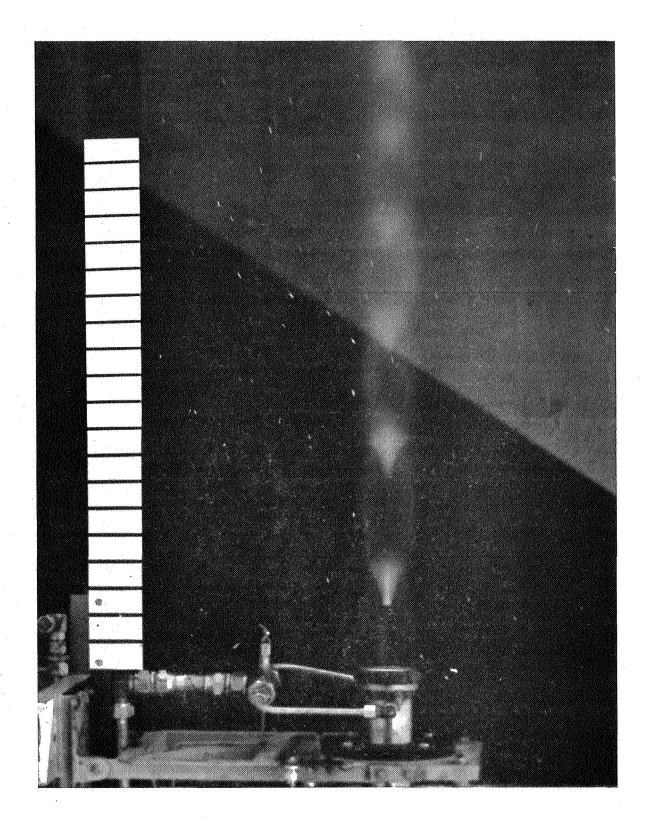
Figure 7 - Test 197-3, LOX-H_2 Exhaust Plume, P_c = 513 psia
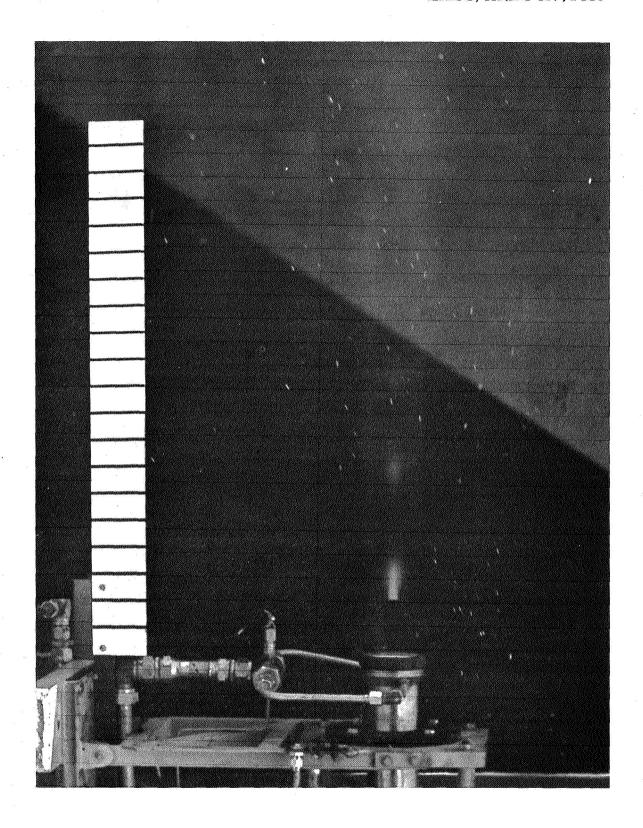
Figure 8 - Test 197-3, LOX-H_2 Exhaust Plume Just Before Engine Cutoff
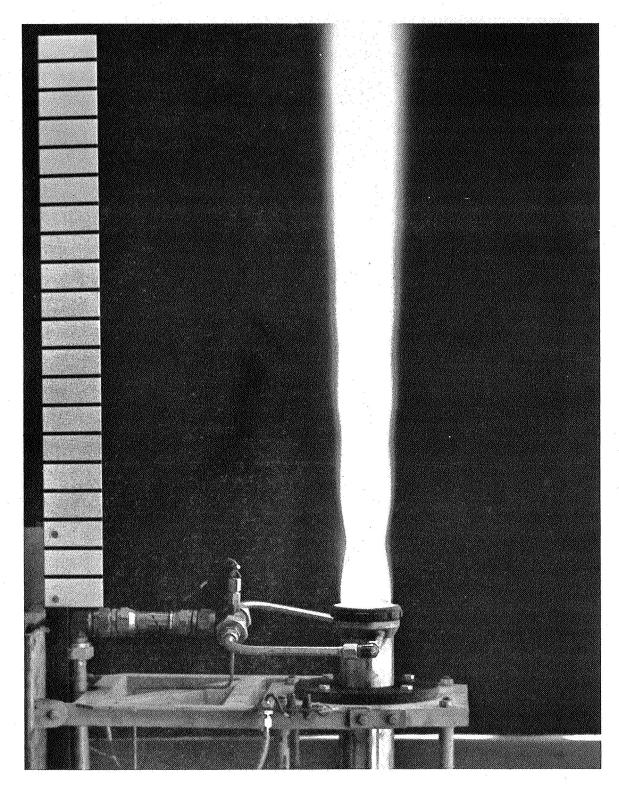
Figure 9 - Test 197-4, Exhaust Plume at Ignition, P_c = 363 psia (Opaque Plume Results from TEA Used for Engine Ignition)
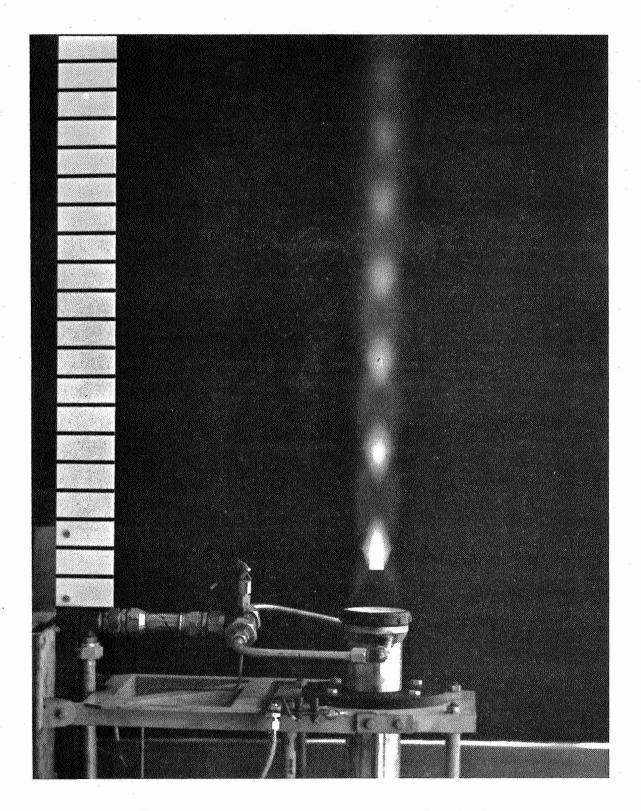
Figure 10 - Test 197-4, Exhaust Plume During Steady State Operation, P_c = 363 psia
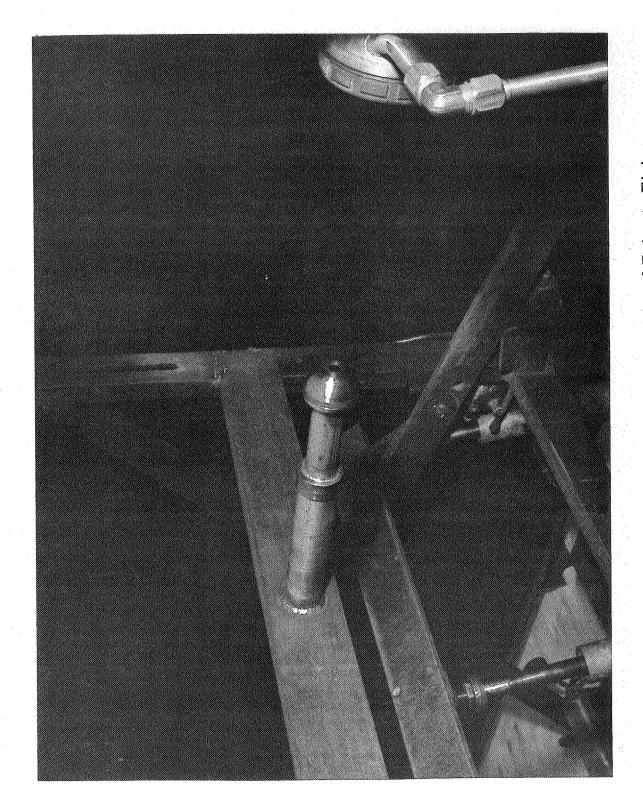
Figure 11 - Test 197-5, Calorimeter Positioned Prior to Firing
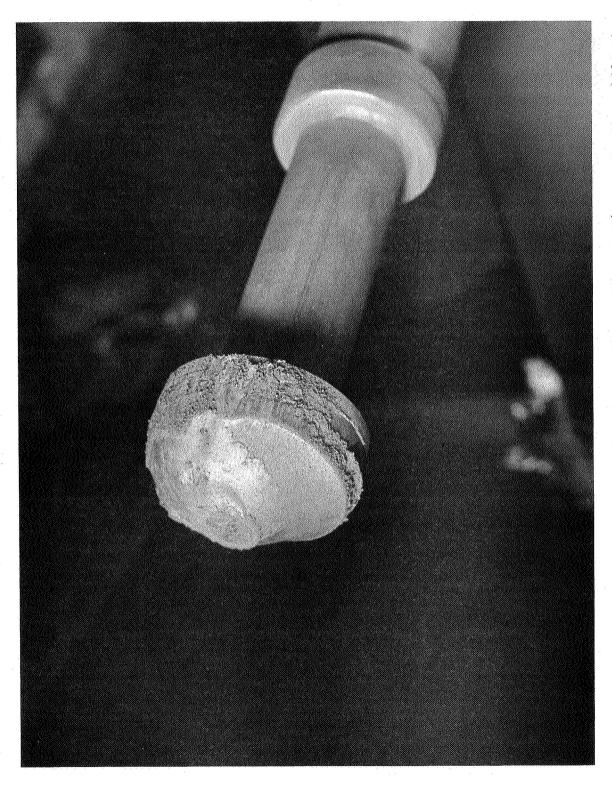
Figure 12 - Test 197-5, Calorimeter After Firing (Firing Time 4.16 seconds, P_c = 343 psia, Axial Distance From Nozzle Exit Plane 8.75 inches)

Figure 13 - Test 197-6, Sample After Firing (Firing Time 2.86 seconds, P_c = 348 psia, Axial Distance from Nozzle Exit Plane 8.75 inches)
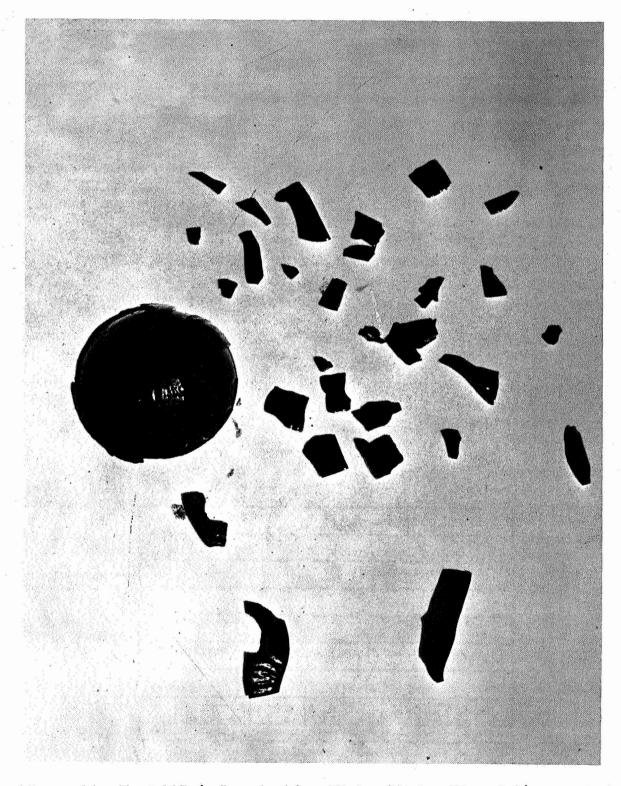
Figure 14 - Test 197-6, Sample After Firing (Firing Time 2.86 seconds, P_c = 348 psia, Axial Distance from Nozzle Exit Plane 8.75 inches)
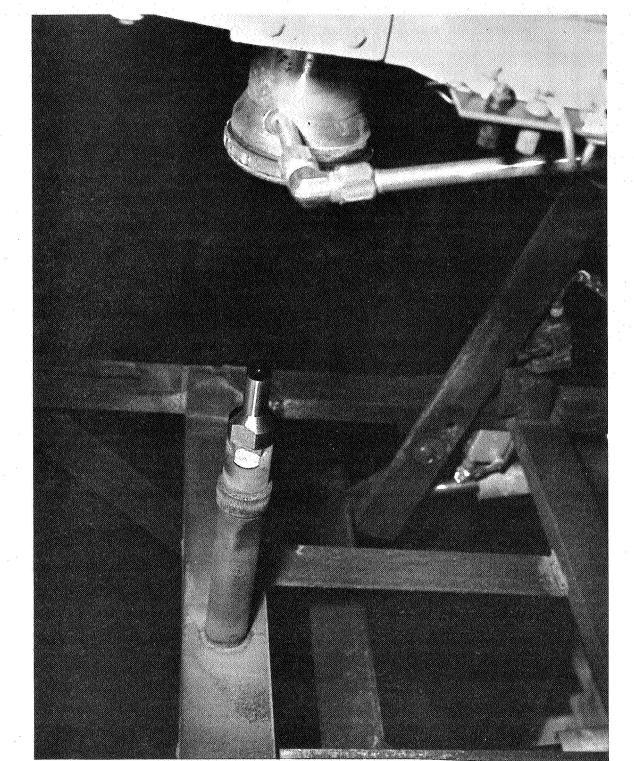
Figure 15 - Test 197-7, Sample Mounted and Ready for Firing
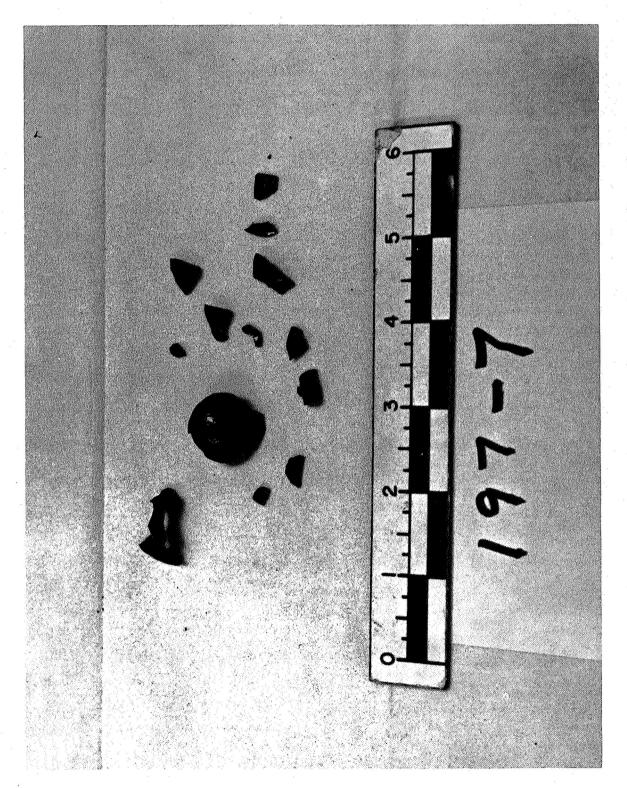
Figure 16 - Test 197-7, Portions of Sample Recovered from Test

Figure 17 - Test 197-8, Sample After Firing.
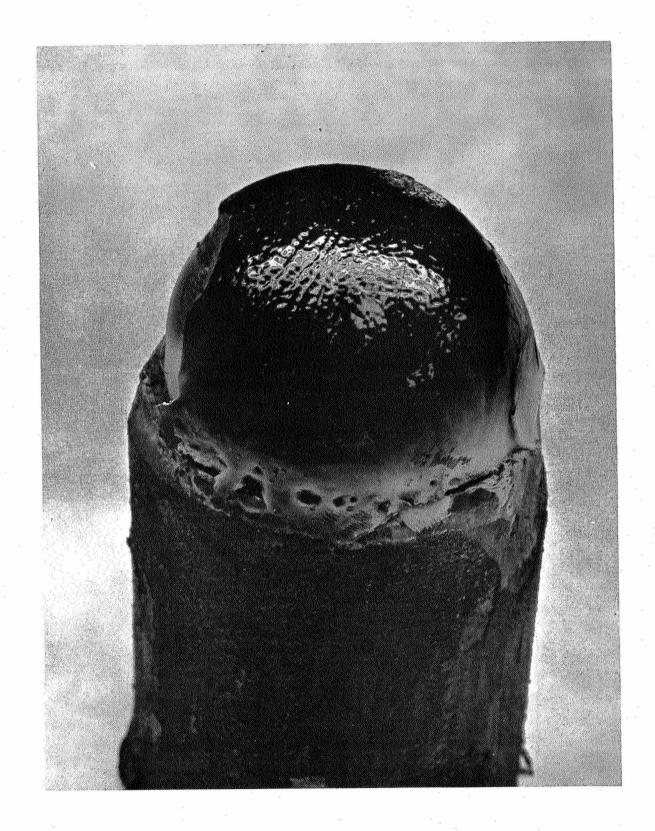
Figure 18 - Test 197-9, Sample After Firing
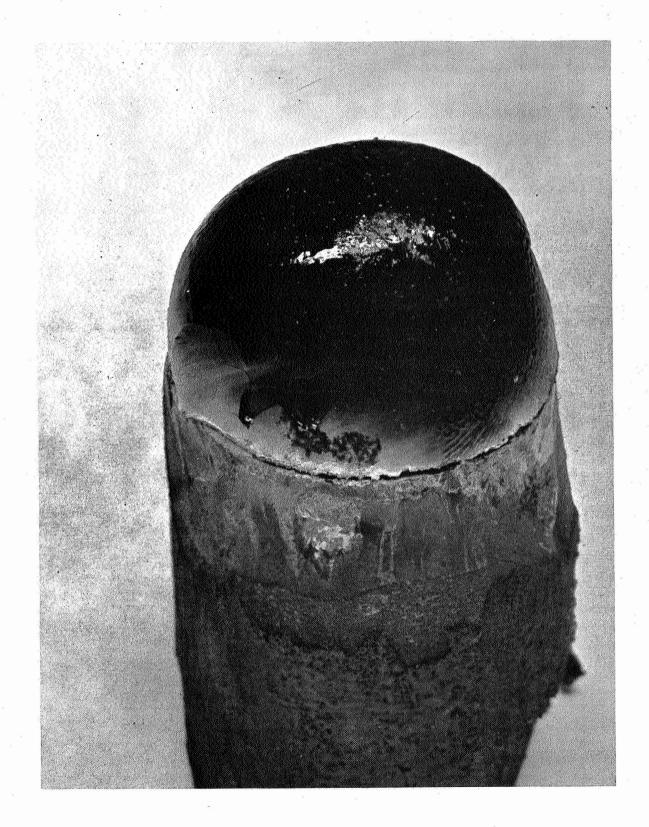
Figure 19 - Test 197-9, Sample After Firing
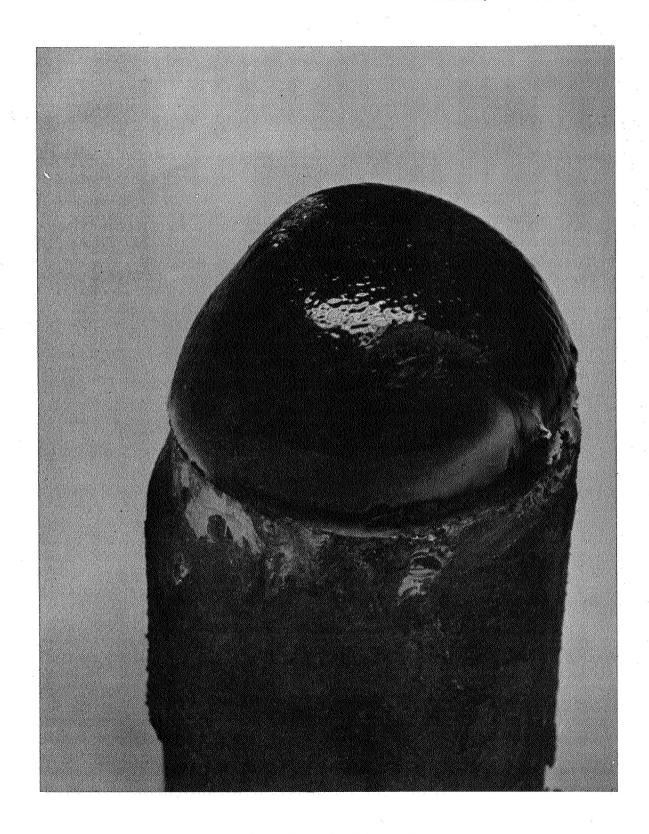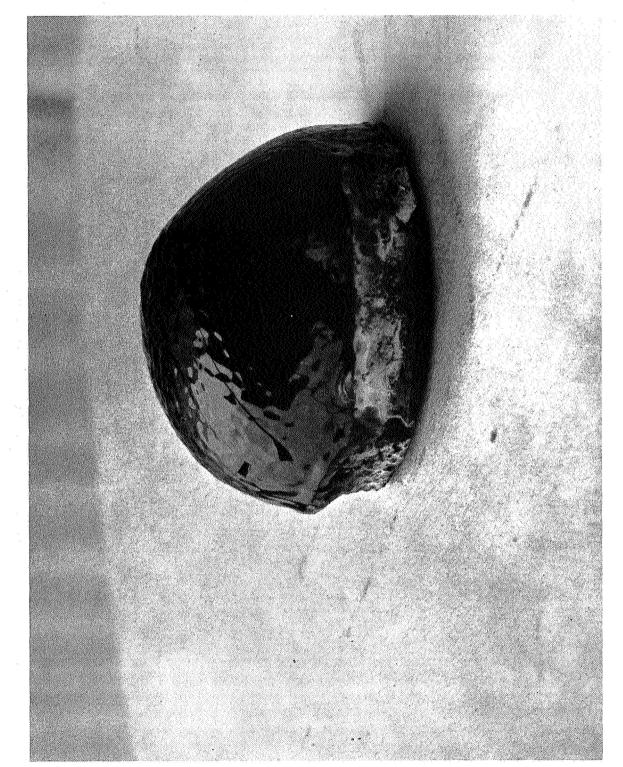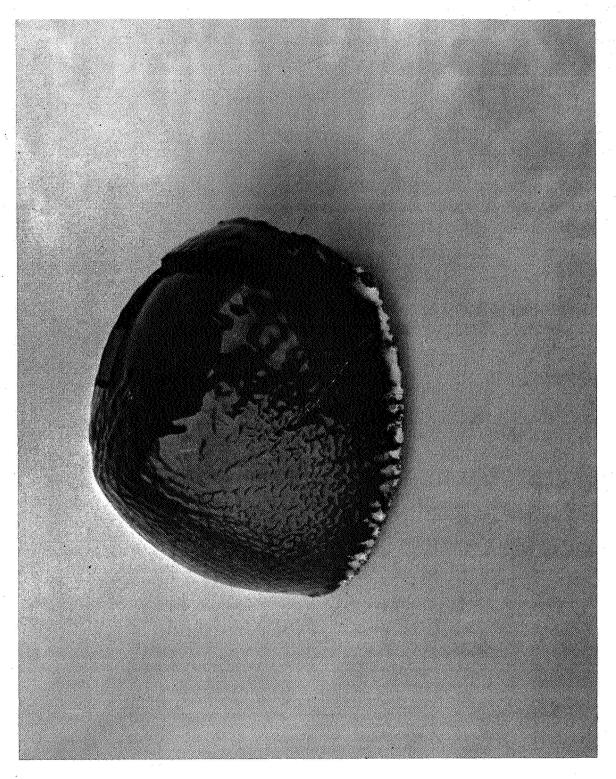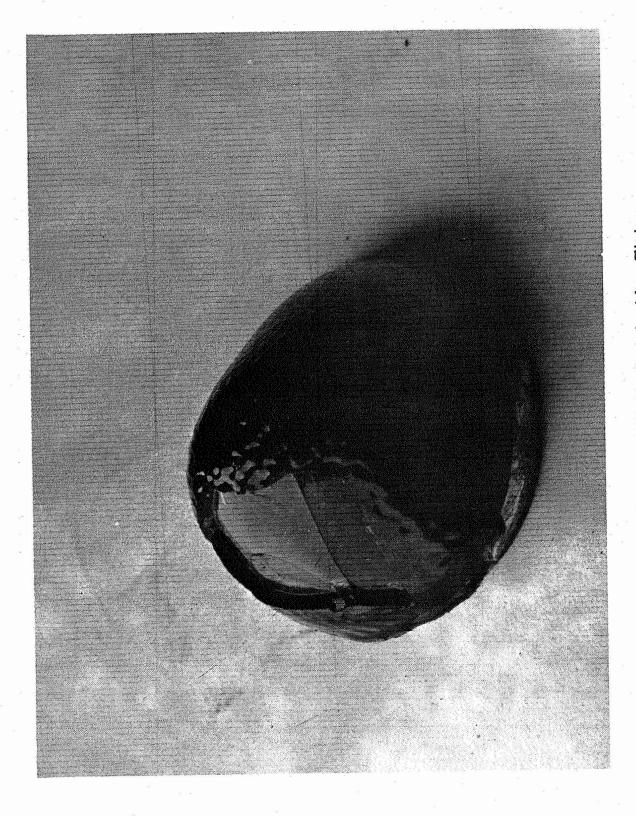
Figure 20 - Test 197-9, Sample After Firing

Figure 21 - Test 197-10, Sample After Firing

Figure 22 - Test 197-10, Sample After Firing

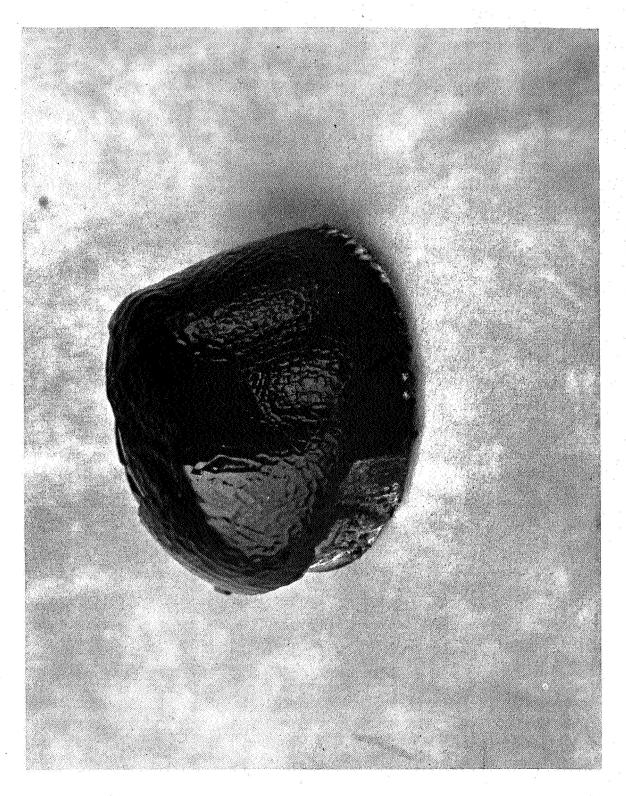Figure 23 – Test 197-10, Sample After Firing

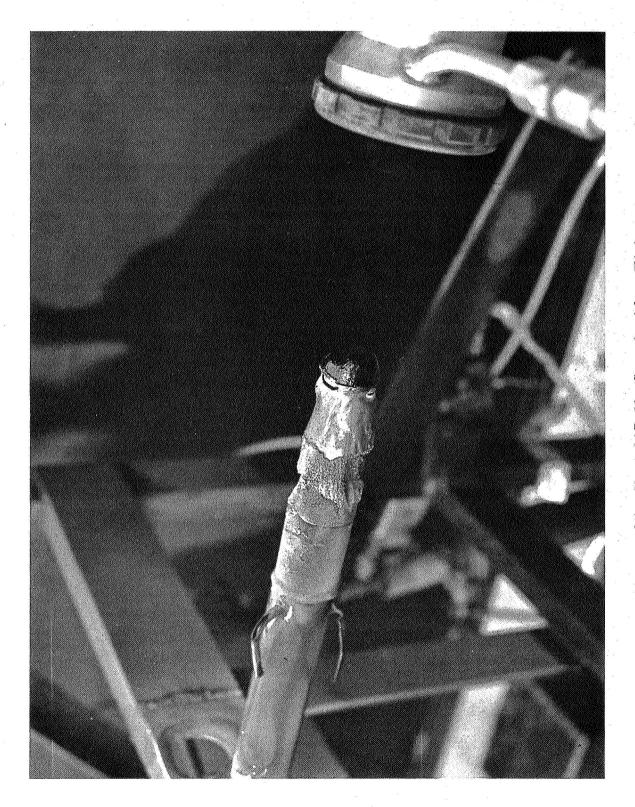Figure 24 - Test 197-10, Sample After Firing
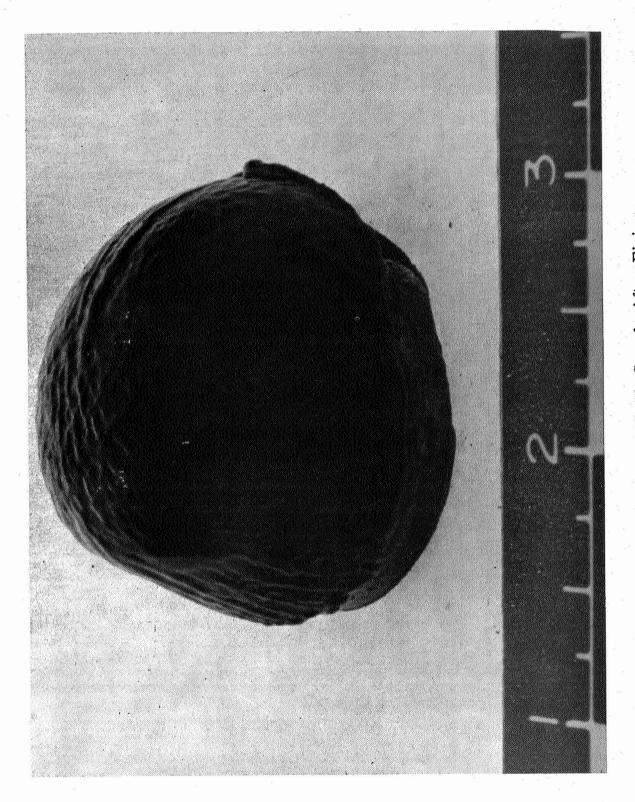
Figure 25 - Test 197-12, Sample After Firing

Figure 26 - Test 197-12, Sample After Firing

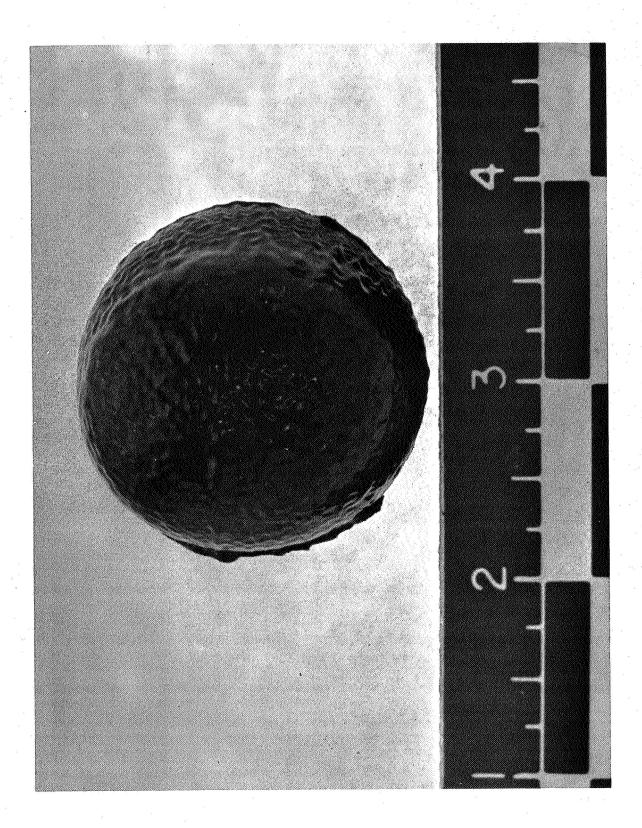Figure 27 - Test 197-12, Sample After Firing

Figure 28 - Test 197-12, Sample After Firing

Appendix A
ANALYTICAL STUDIES AND RECOMMENDED FUTURE EFFORT

SUMMARY

Appendix A

SUMMARY

The purpose of this investigation is to evaluate the surface roughening effects of a high Reynolds number flowfield on glass samples.

With the advent of several rocket exhaust plume high enthalpy test sites, it is possible to simulate a high density entry environment and ensure the somewhat nebulous onset of turbulence over the model due to the inherent vibrations of the nozzle itself. The nozzle chosen for Phase II of this test series was the O_2/H_2 scaled J-2 which is located at the Marshall Space Flight Center, Huntsville, Alabama. The purpose of this appendix is to: (1) document the methods used to understand the environment produced by that facility; (2) make recommendations for testing procedures; and (3) make recommendations for further work.

A.1 DISCUSSION OF ANALYTIC STUDIES

Nature of Test Rocket Flowfield Analysis: The tests were performed by inserting tektite samples into exhaust plumes of existing rocket engines available at Marshall Space Flight Center. The purpose of the analytic evaluation of the test series was to provide meaningful data which would give interpreters of the experiments a basic understanding of the O_2/H_2 exhaust plume. Lockheed/Huntsville through their experience with other high enthalpy rocket test sites (References A.1 through A.3) has evaluated analytically the results of several test series conducted at Lockheed/Santa Cruz, and General Electric/Malta. Using an approach similar to those documented in the above references the following study was performed.

Definition of O_2/H_2 Rocket Exhaust Plume: Because of the test plan
of initially firing engines at low operational chamber pressures and then
increasing the pressure settings with each test shot, a series of plumes at
various engine chamber pressures was calculated using the Lockheed
Method-of-Characteristics Computer Program (Reference A.4). Chamber
pressures of 350, 750, and 1000 psia were selected with an oxidizer to fuel
ratio equal to 5.5. These conditions produce approximate equilibrium gas
compositions of steam and molecular hydrogen at the exit plane of the rocket
engine in mole fractions equal to 0.69 and 0.31, respectively, as calculated
by the method of Reference A.5. A presentation of the plume flow character-
istics for the 750 psia analysis is made in Figure A-1, where the flow Mach
number, Reynolds number and flow angle are plotted as a function of distance
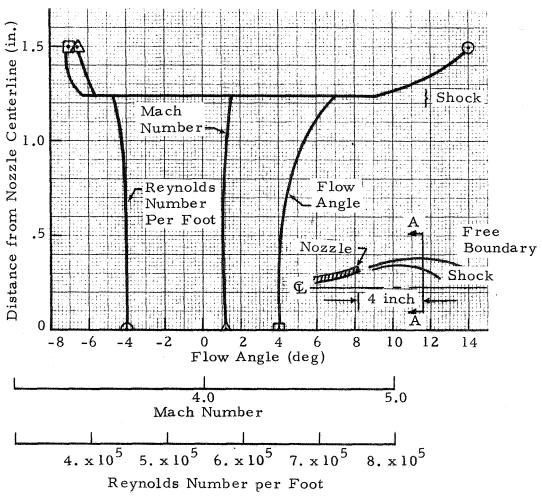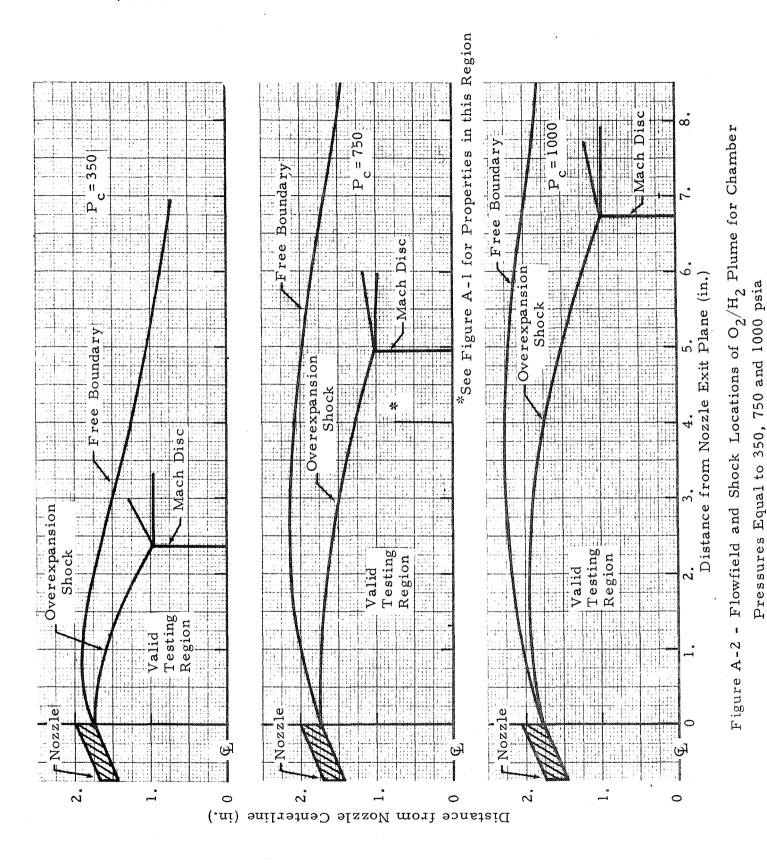from the nozzle centerline for the nozzle exit plane plus four-inch station in

Figure A-1 - Flow Field Properties at Exit Plane Plus Four-Inch Station
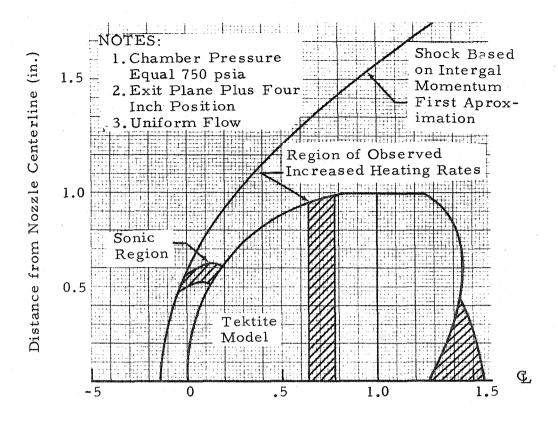for Chamber Pressure Equal 750 psia

A-2

the plume. The discontinuity at the 1.24-inch radial location is caused by the shock produced as the overexpanded plume seeks to match the surrounding atmospheric conditions. This same phenomenon also creates a normal shock (Mach disc) in the flowfield as located for each plume and presented on Figure A-2. The oblique overexpansion shock and the Mach disc are clearly labled, and ideally for any meaningful test to freeflight data match, the model should be located upstream of these two shocks. Although the first tests were operated with the models well downstream of the first Mach disc, the ideal situation was approached during the latter portion of the test series. The latter portion of the test series produced the best tektite roughening results. It is also noted that the flow is slightly diverging (Figure A-1, flow angle) which also leads to a slightly different environment other than that expected under freeflight conditions. The Mach discs were located by the methods of References A.6 and A.7 which have been extensively investigated and compared to test data by the authors of Reference A.8. The final flowfield as produced by the nozzle for the 750 psia chamber pressure conditions proved to be quite satisfactory for the type of flow needed for successful ablating tektite tests.

Existence of Turbulent Flow on Model: The use of the O_2/H_2 scaled J-2 engine to produce the turbulent boundary layer, as would be encountered during a parent body originated entry, is justified both by classic calculations of conditions necessary for turbulence, and by rocket test site phenomena which produce early onset of turbulence. The body flow field was calculated by the method of integral relations (Reference A.9) and both laminar and turbulent boundary layers were calculated about the models by the method as suggested by Reference A.10. Results depicting the shock structure and heating rate levels expected for the 750 psia test case are presented in Figure A-3. A calculation of momentum thickness Reynolds number transition criteria (Reference A.11) shows that transition from laminar to turbulent flow should occur at approximately 70 degrees from the model stagnation point. At this location on the models, the test photography showed that the transient glowing of the models during the initial seconds of the test runs reached a peak intensity. This could be directly attributed to the high heating rates associated with the turbulent boundary layer.

In addition to the above study, it has been Lockheed/Huntsville's experience that the heating rates produced on models placed in similar flowfields are

Figure A-2 - Flowfield and Shock Locations of O_2/H_2 Plume for Chamber Pressures Equal to 350, 750 and 1000 psia
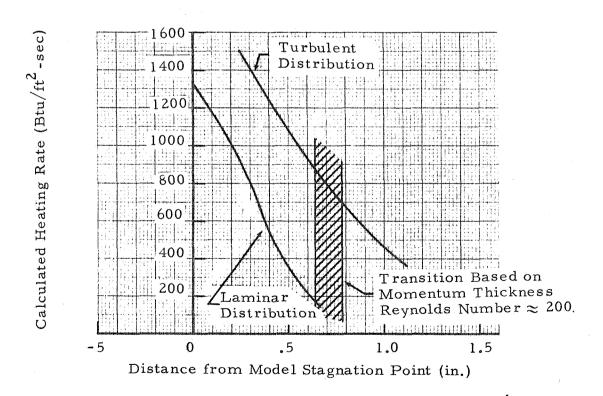
Figure A-3 – Tektite Model Flow Field and Transition Location

also turbulent in nature. This turbulence is impressed over the entire nose-cap by the noise vibrational levels and detonating wave formations of the rocket combustion process. This is illustrated graphically in Figure A-4 and has been the center of a so-called "Cross hatching" controversy over the past several years. Examples of these effects on several test programs are reported in References A-12 through A-14 as well as in the References A-1 through A-3.

Regardless of the mechanism of the onset of turbulence, it is evident that the high density nozzle flow field available at the O_2/H_2 test stand does produce the environment necessary for simulation of a high density, low altitude entry. Therefore, the surface structure observed on the tested tektite samples was produced by the high density turbulent flow environment.

A.2   RECOMMENDATION OF FUTURE THEORETICAL STUDY AND
         SUPPORTING MODEL TESTING

• Redesign of Model Sting and Shield: Although valuable insight into the tektite surface structure problem was gained during this test series, the model location in the O_2/H_2 exhaust plume was less than satisfactory. This was due to the arrangement of the flame deflector shield which did not allow mounting of the test samples upstream of the first Mach disc. Therefore, it is recommended that for future tests this shield be redesigned for a test series in which the location of the model is in the most favorable position for simulation of the tektite entry environment.

• In-Depth Comparison of Theory to Tektite Data and Data from Cross-Hatching Test: Data were generated on the pitting of tektites experimentally and analytically during this test series. Budget restrictions, however, prohibited a wide literature search that would have allowed comparison with observed similar phenomena at other facilities. There have been several other occurrences of the pitting (cross hatching) both on flight reentry hardware and in ground tests. In all instances similar pitting does not occur without the high density turbulent boundary layer environment. With this in
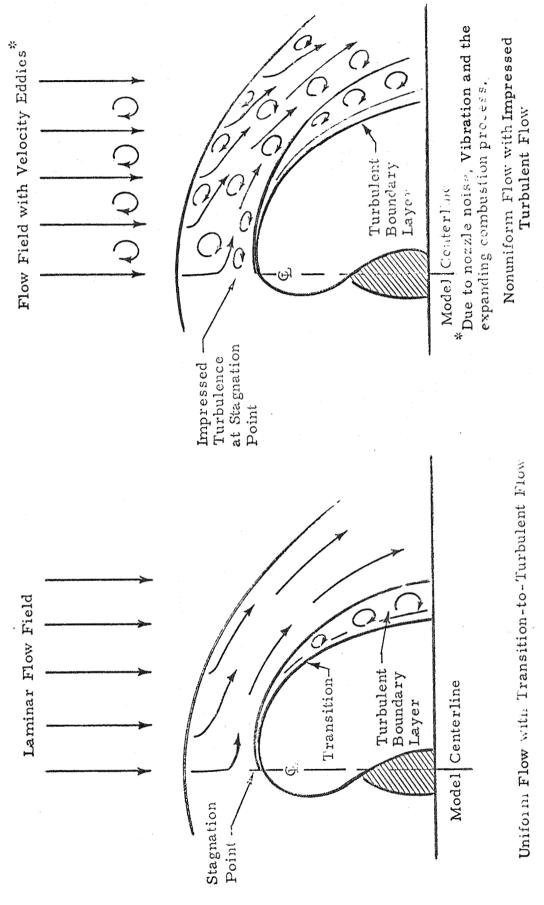
Figure A-4 - Schematic Comparison of Difference Between Uniform Flow Field and Flow Field Containing Turbulent Eddies

mind, the existence of pitting during the parent body entry seems to have valid substantiation with the test information now at hand. This area should be investigated further.

• <u>Further Proof of Turbulent Flow with Calibration Model Test</u>: Lockheed/ Huntsville, upon observing the hot ring about the transition zone on the tektite models, recommended a calibration model test which would define the actual heating rate distribution over the tektite model. To this end, a water-cooled calibration model was prepared (shown in Figure A-5) with the slug calorimeters. This model was to be mounted and calibrated by Lockheed personnel for this investigation. This test, however, was not completed during the current program due to time and budget limitations. It is felt that the overall favorable results of the completed test program warrent further testing with this calibration model as a primary specimen. This would further support the argument for turbulent flow (turbulent heating rate distribution) over the test specimens.

A.3 CONCLUSION

From the analysis performed during the course of the experimental work, it is evident that the flowfield does reproduce the high Reynolds number entry environment. Additional data from other test series show that pitting is associated with turbulent boundary layer growth on nosecaps. Meaningful data was generated during the analysis and test period; however, further effort would seriously enhance the relationship of the tektite surface structure problem to the parent body hypothesis.
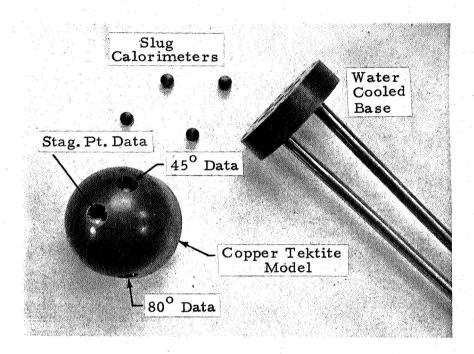
Figure A-5 - Photograph of Water-Cooled Tektite Calibration Model

PRECEDING PAGE BLANK NOT FILMED.

REFERENCES

A.1 Blackledge, M.L., "Flowfield Characteristics of the Malta Pit Four LOX/Alcohol Rocket Exhaust Plume and its Heating Rate Effects on the AM-1 and M-1 Reentry Configurations (U)," LMSC/HREC A783904, Lockheed Missiles & Space Company, Huntsville, Ala., February 1967 (Confidential).

A.2 Blackledge, M.L., "Analysis of M-1 Reentry Vehicle as Tested at the Malta and Agena Rocket Exhaust Facilities (U)," LMSC/HREC A783892, Lockheed Missiles & Space Company, Huntsville, Ala., January 1967 (Confidential).

A.3 Blackledge, M.L., "Final Report, Malta AM-1 Test Series (U)," LMSC/ HREC B033607, Lockheed Missiles & Space Company, Huntsville, Ala., May 1967 (Secret Restricted Data).

A.4 Prozan, R.J., "Development of a Method-of-Characteristics Solution for Supersonic Flow of an Ideal, Frozen or Equilibrium Reacting Gas Mixture," LMSC/HREC A782535, Lockheed Missiles & Space Company, Huntsville, Ala., April 1966.

A.5 Zeleznik, F.J. and S. Gordon, "A General IBM 704 or 7090 Computer Program for Computation of Chemical Equilibrium Compositions, Rocket Performance, and Chapman-Jouget Detonations," NASA TN 1454, Lewis Research Center, Cleveland, Ohio, October 1962.

A.6 Eastman, D. and L. Radtke, "Two-Dimensional or Axially Symmetric Real Gas Flows by the Method of Characteristics, Part III: A Summary of Results from the IBM 7090 Program for Calculating the Flow Field of a Supersonic Jet," Boeing Company Report 02-10599, December 1962.

A.7 Bowyer, J., L. S'Attore and H. Yoshihara, "Transonic Aspects of Hyper-velocity Rocket Plumes," Supersonic Flow, Chemical Processes and Radiation Transfer, Edited by D.B. Olfe and V. Zakkay, Pergamon Press, pp. 201-210, 1964.

A.8 Farmer, R.C., R.J. Prozan, L.R. McGimsey and A.W. Ratliff, "Verification of a Mathematical Model which Represents Large Liquid Rocket Engine Exhaust Plumes," AIAA Paper No. 66-650, 13 June 1966.

A.9 Belotserkovskii, O.M., "On the Calculation of Flow Past Axisymmetric Bodies with Detached Shock Waves Using an Electronic Computing Machine," PMM Vol. 24, No. 1, pp. 511-517, 1960.

A.10 Vaglio-Laurin, R., "Supersonic Flow About General Three-Dimensional Blunt Bodies," ASD-TR-61-727, Vol. 1, FDL Wright-Patterson Air Force Base, Ohio, October 1962.

A.11 Blackledge, M.L. and C.J. Wojciechowski, "Real Gas Multiple Pressure Gradient Heating Rate Program," LMSC/HREC A783781, Lockheed Missiles & Space Company, Huntsville, Ala., May 1967.

A.12 General Electric Company, "Calibration Model Test Data Report – Avco Corporation," TM 5250-67-36, General Electric Company Ballston Spa, N.Y., 4 December 1967.

A.13 Canning, T.N., M.E. Wilkins, and M.E. Tauber, "Ablation Patterns on Cones having Laminar and Turbulent Flows," AIAA J., Vol. 6, No. 1, p. 174, January 1968.

A.14 Tauber, M.E. and M.E. Wilkins, "Boundary Transition on Ablating Cones at Speeds up to 7 km/sec," AIAA J., Vol. 4, No. 8, p. 1344, August 1966.

APPENDIX B

SOURCES OF TEKTITE SAMPLES

Appendix B

Source of Natural Tektite Samples

Dr. John A. O'Keefe of Goddard Space Flight Center supplied the natural tektite samples used in the Phase I investigation.

Synthetic Samples

The one- and two-inch synthetic tektite samples were obtained from Dr. John A. O'Keefe. They had an overall chemical composition approximating that of natural tektite materials.